



# Spatio-temporal analysis of rural–urban transitions and transformations in Gautam Buddha Nagar, India

S. S. Somvanshi<sup>1</sup> · M. Kumari<sup>2</sup> · R. Sharma<sup>2</sup>

Received: 20 August 2022 / Revised: 14 August 2023 / Accepted: 31 October 2023 / Published online: 22 November 2023

© The Author(s) under exclusive licence to Iranian Society of Environmentalists (IRSEN) and Science and Research Branch, Islamic Azad University 2023

## Abstract

In recent decades, exponentially expanding population and urbanization have prompted an unplanned and unsustainable urban sprawl, an emerging major threat in developing countries. Temporal examination of land-use/land-cover (LULC) and the identification of transition zones are vital for the sustainable improvement of the city. Therefore, an appropriate methodology is needed to critically analyse the degree, causes and effects of urbanization. This paper analyses the spatio-temporal dynamics of the urbanization process in Gautam Buddha Nagar, one of the important cities of Ganga alluvial Plain. The study quantitatively evaluates the extent, direction and growth of urbanization with Landsat data of year 2001, 2010 and 2016. Urbanization's magnitude, trajectory and expansion were assessed quantitatively in this study using Landsat data from 2001, 2010, and 2016. To determine the changes and trends, LULC categorization maps were generated from 2001 to 2016. A micro-level urban footprinting analysis was carried out on the basis of urban densities and was classified in seven sub-categories (i) urban built-up, (ii) suburban built-up, (iii) rural built-up, (iv) urbanized open land, (v) captured open land, (vi) rural open land, and (vii) waterbody. The results of the urban landscape quantification and transition points were also compared with land surface temperature (LST) indicating overall rise in LST over the time.

**Keywords** LULC characterization · Land surface temperature (LST) · Rural–urban transition · Urban land dynamics · Urban footprinting

## Introduction

Urban sprawl is a process that is dynamic and socio-economic in nature whereby rural areas are transformed into urban areas (Jat et al. 2008). This process does not only manifest itself through an increase in land ceiling but also gradually changes the identity of the social and physical landscape from a rural to an urban character. India is expected to undergo major rural–urban transitions in the coming years. Numerous studies have quantified and analysed the scope and consequences of rural–urban changes. (Mushore et al. 2017; Tang et al. 2007). The national spatial policy of India

does not qualify nor specify where urban boundaries are located or where and how cities may expand (Fazal 2000; Jiang et al. 2007). The immediate result of this absence of boundary specifications is an unsustainable urban growth at the expense of surrounding rural territories and/or vacant lands, leading to unplanned and uncontrolled urban sprawl (Zhao et al. 2019). Additionally, this leads to an exponential increase in what can be referred to as peri-urban city boundaries characterized physically by decreasing areas of cropland and increasing areas of urban built-up and land ceiling (Anane 2022; Anugya et al. 2017). These physical changes also inflict considerable changes in the economic opportunities and possibilities, which are often manifested in loss of employment for farmers or changing socio-economic status of individual and communities in these areas of transition.

Presently, the majority of Indian cities are undergoing this shift, which is eventually having a negative impact on the rural–urban income disparity throughout the nation. (Bhatta et al. 2010; Stone et al. 2010). In other words, there is an increase in spatial inequality, visible in the amount and types of economic opportunities and

Editorial responsibility: S. Mirkia.

✉ M. Kumari  
maya.84s@gmail.com

<sup>1</sup> Amity Institute of Environmental Sciences, Amity University, Noida, Uttar Pradesh, India

<sup>2</sup> Amity School of Natural Resources and Sustainable Development, Amity University, Noida, Uttar Pradesh, India



dependencies in rural areas, a decrease in public services in rural areas, and decline in rural identities (Guo and Zhong 2023; Martinuzzi et al. 2007). On top of that, food security is at risk, given the huge decline in arable land and the rural workforce (Ren et al. 2013). In order to address and get a grip on these critical developments, there is an urgent need to continuously monitor and identify the growth of the transition areas, and the effect of the urbanization (Kassouri and Okunlola 2022; Sudhira et al. 2004; Zhang et al. 2023). Although it is obvious that these rural–urban transitions have negative effects on the various aspects of both the city and the rural areas, it is currently unclear how significant these effects are and what kind of effects they are specifically. (Cheng and Masser 2003; Dhanaraj and Angadi 2022). The current knowledge is that the transformations tend to result in spatial ambiguity in areas that are unplanned and where fragmented LULC patterns emerge (Ji et al. 2006; Kumar et al. 2007).

Some of the outlying rural communities transform into (peri) urban areas or urban villages as urbanization spreads, while others retain their rural character. (Balha and Singh 2018). However, the amount and direction of this spatial difference are not always obvious. As a result, additional spatiotemporal data are necessary for quantifying, mapping, and monitoring large-scale land modification. (Lillesand and Kiefer 1979; Niyogi et al. 2018). It has proven effective for improving monitoring and analysis of urban land transitions and changes, as well as urban land dynamics (Tsai 2005). Based on the findings of these studies, it is evident that urban heat islands (UHIs) result from the increased land surface temperature linked to the ceiling of rural lands (including agricultural and forestry lands) (Jeganathan et al. 2016). Recent advances in thermal remote sensing, GIS and statistical methods have helped researchers carry out studies to analyse, monitor and map the location and severity of these UHIs. These insights have significantly contributed in policy formulation procedures for a more sustainable urban development (Chen et al. 2006; Kumari and Sarma 2017; Roy and Kasemi 2021).

Given this context, this study aims at critically analysing both the physical and spatial rural–urban transitions as well as the environmental parameters associated with it them, for a particular study area. The spatio-temporal characteristics of both types of transitions relied on geospatial and statistical methods. Therefore, the primary focus of the study is:

- (1). To evaluate the area change associated with the urban growth of the GBN district between 2001 and 2016.
- (2). To determine the urban footprint in view of built-up densities and its relation with land surface temperature of the area. These outcomes establish a framework for additional examination on rural–urban transition in an applied manner

## Study area

The district of Gautam Buddha Nagar (GBN), which has geographic coordinates of longitude 77°17'–77°45' E and latitude 28°5'–28°41' N, is one of the major cities in the National Capital Region (NCR). The study area is 1442 square kilometres and is located in the Indo Gangetic Plain at an altitude of about 200 m above mean sea level. With an average precipitation of about 790 mm, the climate varies from sub-humid with hot summers to cold winters (Fig. 1). The most common crops are wheat, rice, mustard, barely, sugarcane and maize. From 8,38,469 in 1991 to 16,48,115 in 2011, the population of the GBN has significantly increased over the past 20 years.

## Materials and methods

### Data sources

The temporal Landsat satellite images with the spatial resolution of 30 m acquired in 2001, 2010 and 2016 were used for thematic layers' preparation along with the field data collection. The accuracy assessment was done through waypoints using Oregon 550 GPS handheld receivers. The utility

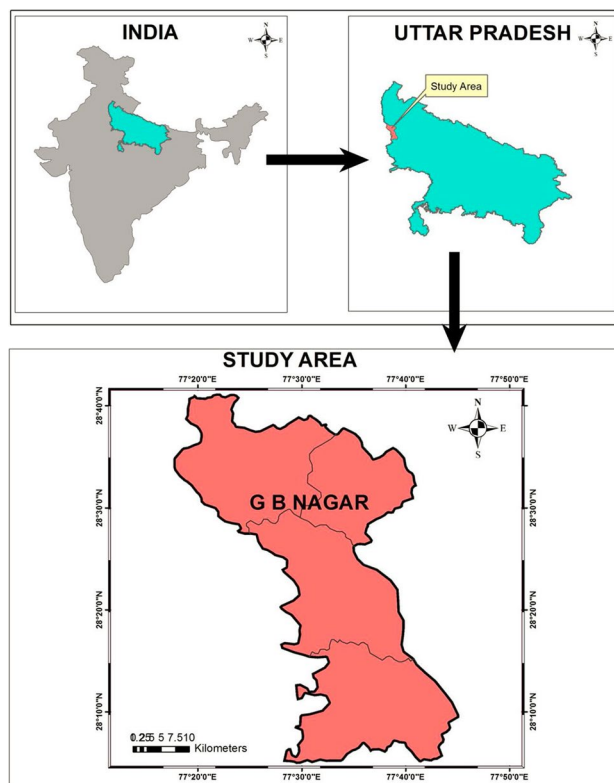


Fig. 1 Location map of study area



of thermal band for deriving the temperature was utilized to investigate the variation in temperature of the area due to expansion in urban settlement. The UTM (WGS-84) coordinate system was used to reproject all the images, harmonizing the various data sets and making them comparable for spatial analysis. Hyperspherical shading space (HCS) fusion and low-pass spatial filtering were used to improve the images (Somvanshi and Kumari 2020). The details of the data are displayed in Table 1.

### LULC characterization

Satellite images from 2001, 2010, and 2016 were classified under supervision using the Mahalanobis classifier algorithm (Somvanshi et al. 2020). This research concentrated on three main classes: built-up, waterbody, and others. Built-up areas include all surface areas that have been developed, including all paved or rocky surfaces, buildings, and other infrastructure. The waterbody category comprises of flowing waterbodies (rivers and streams) and stagnant waterbodies (ponds, lakes and waterlogged). The agriculture, vegetation, fallows land, forest, and open spaces were counted in others

**Table 1** Satellite data specification

Satellite	Sensor	Path	Row	Date of acquisition	Spatial resolution (m)
Landsat 5	TM	146	40	05/02/2001	30/120
Landsat 5	TM	146	40	14/02/2010	30/120
Landsat 8	OLI/TIRS	146	40	02/03/2016	30/100

class. To validate the accuracy of LULC maps of 2001, 2010 and 2016 (Fig. 2), the accuracy of classified images was assessed using error matrix at producer, user and overall accuracy levels (Congalton 1991; Stabursvik 2007).

### Urban landscape quantification

To analyse the spatial expansion of the urban landscape classification was done for three time periods, namely 2001, 2010 and 2016. The quantification was done according to rule-based categorization scheme (Angel et al. 2007). Urban densities were analysed grid wise by dividing the entire study area into grids. Each grid comprises of an area 4 km sq. (2 km × 2 km). The developed (built-up extent and density) and non-developed (rural area) category were assigned on the basis of the urban density values. Urban density estimation parameters were derived from the compactness and association of urban pixels. Furthermore, for the footprint mapping, the sub-categories (urban built-up area, suburban built-up area, rural built-up area, urbanized open land (UOL), captured open land (COL), rural open land (ROL) and waterbody) were assigned on the basis of extent and density of built in each grid, or in other words, the percentage of total built-up area in each grid. The developed and undeveloped lands were calculated using Eqs. (1, 2).

$$U_b = [UB_i/TA] * 100 \quad (1)$$

where  $U_b$  is extent and density of the built-up area,  $UB_i$  is the total urban built-up area in a grid, and TA is the total area of the grid.

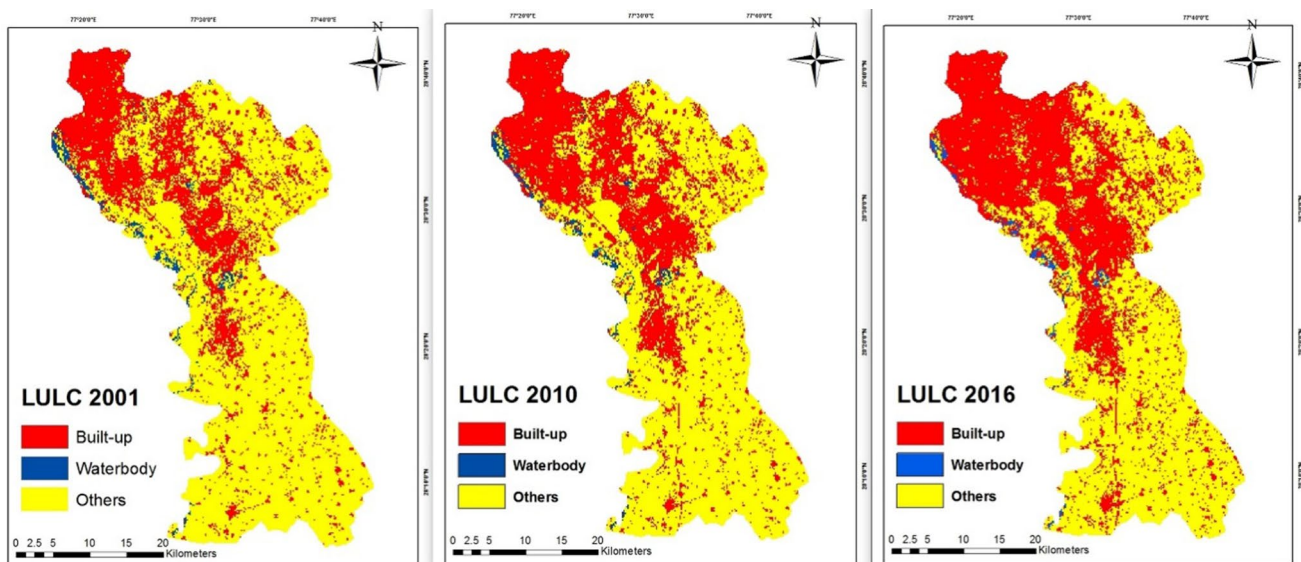


**Fig. 2** LULC classification map **a** 2001, **b** 2010 and **c** 2016

The dynamics of urban landscape is estimated on the basis of value of  $U_{ud}$ .

$$U_{ud} = [U_{udi}/TA] * 100 \tag{2}$$

where  $U_{ud}$  is extent and density for the undeveloped area,  $U_{udi}$  is the total undeveloped area in a grid, and TA is the total area of the grid. Parameter used for identifying unsustainable sprawl is decreasing spatial extent and density of developed land as the physical fragmentation of built-up areas increases and also an increase in isolated urbanized patches.

### Urban footprint mapping

The Urban footprint map of the study area was generated by classifying into seven sub-categories which were the urban area, Sub-urban area, Rural area, UOL, COL and ROL (Table 2).

Pixel values were assigned based on the extent and density of urban areas.  $U_b > 50\%$  was an urban built-up area, 10–50% was a suburban one, and 10% was a rural one (Fig. 3). Similar to how pixel value was assigned for developed land, the extent and density of undeveloped land were taken into account. Areas with a  $U_{ud}$  value greater than 50% were classified as UOL, while areas with a  $U_{ud}$  value of less than 200 ha that were surrounded by urban and suburban patches were classified as COL.

### Land surface temperature estimations

The methodology for deriving the LST was in accordance with LANDSAT Science Data Users Handbook.

Spectral radiance ( $L_\lambda$ )	$L_\lambda = \text{gain} \times \text{DN} + \text{offset}$ Where $L_\lambda$ is the spectral radiance, DN is the digital number of a given pixel, gain is the slope of the radiance/DN conversion function, and offset is the intercept of the radiance/DN conversion function
-----------------------------------	---

Brightness temperature	$T_B = K_2 / \left( \ln \left( \frac{K_1}{L_\lambda} \right) + 1 \right)$ In this equation, $T_B$ represents the brightness temperature in kelvin, $K_1$ represents calibration constant 1, $K_2$ represents calibration constant 2, and $L$ represents the spectral radiance of thermal band pixels
Land surface emissivity (LSE)	$LSE = 0.004P_v + 0.986$ Where $P_v$ is proportionate vegetation
Land surface temperature (LST)	$LST = \frac{T_B}{1 + \left( \frac{2T_B}{\rho} \right) \ln \epsilon}$ Where $\lambda$ is the wavelength of the emitted radiance; $\rho = h * c / \sigma$ (1.438 9 10–2 Mk); $\sigma$ is Boltzmann’s constant (1.38 9 10–23 JK <sup>-1</sup> ); $h$ is Planck’s constant (6.626 9 10–34 Js), and $c$ is the velocity of light (2.998 9 108 ms <sup>-1</sup> )

## Results and discussion

### LULC characterization

According to the spatio-temporal analysis of LULC, the built-up area was 396.59 sq km in 2001 and then rose to 594.82 sq km in 2016. The built-up area increased from 27.51 per cent of the total area in 2001 to 41.25 per cent in 2016. Over the course of 15 years, this increase in built-up area resulted in a 13.13 per cent decline in agricultural land and other classes. As shown in Table 3, the conversion of arable land took place during the development phase. Along the main roads and highway network, significant urban expansion was seen.

### Accuracy assessment

In order to evaluate the effectiveness of Mahalanobi’s classifier in urban mapping and the accuracy of categorized

**Table 2** Urban footprint classification

Sub-categories	Characteristics
Urban area	The dense urban built-up with surrounding neighbourhood pixels more than 50%
Sub-urban area	the region with at least 10–50% of the surrounding pixels being built-up cities (Not a part of the downtown area)
Rural area	The region outside of cities and suburbs where less than 10% of the pixels are built-up
UOL	Characterized as urbanized patches of open land encircled by urban and suburban areas
COL	Less than 200 ha of the undeveloped patches are completely encircled by urban, suburban, and UOL areas
ROL	The undeveloped region outside of the UOL and COL



**Fig. 3** Urban footprint maps of 2001, 2010 and 2016

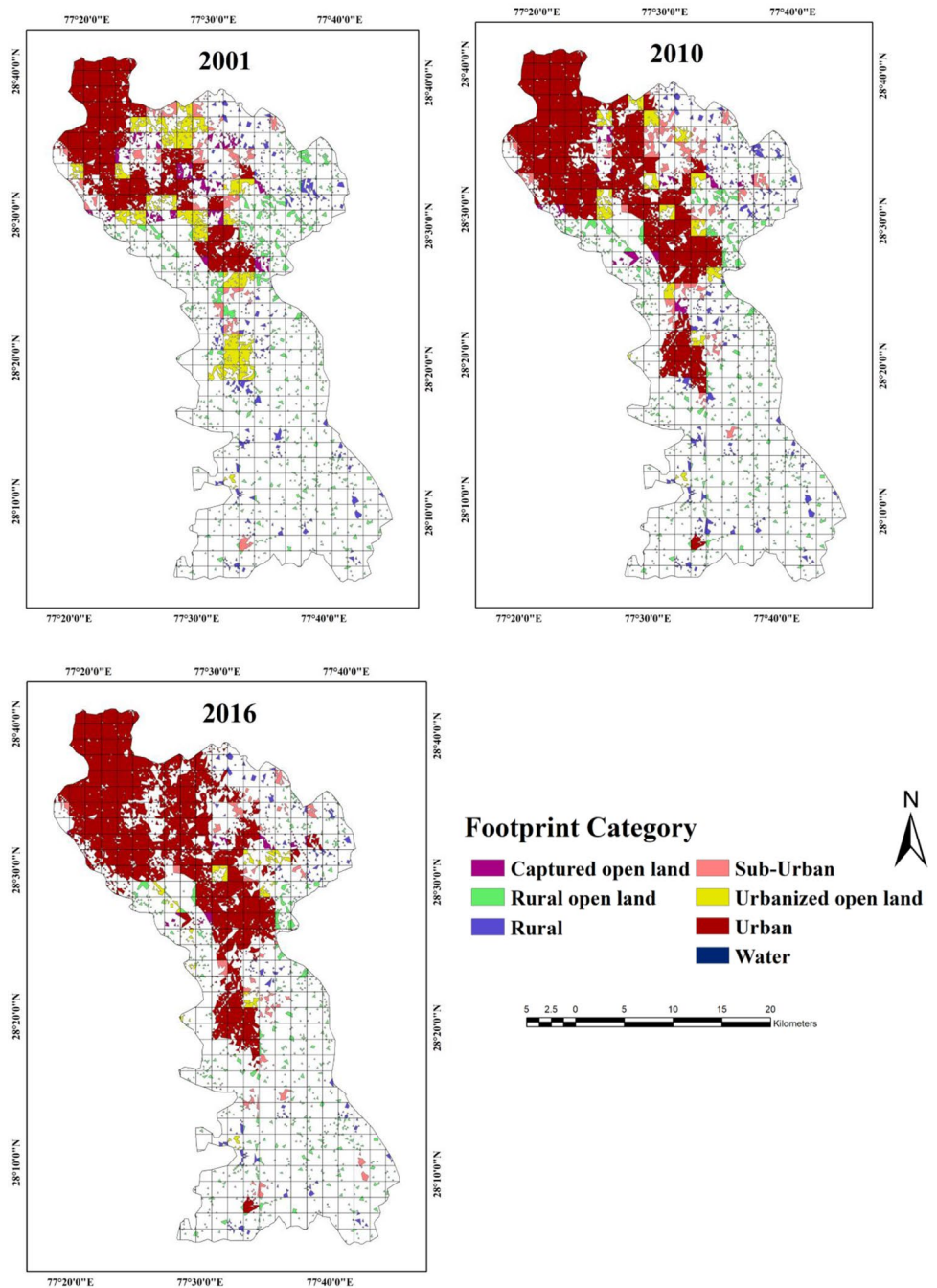


**Table 3** Spatio-temporal LULC classification statistics

S. no	LULC class	2001		2010		2016	
		Area (sq. km)	Area (%)	Area (sq. km)	Area (%)	Area (sq. km)	Area (%)
1	Built-up	396.59	27.51	486.27	33.73	594.82	41.25
2	Water body	24.21	1.69	22.70	1.57	15.57	1.08
3	Others	1021.20	70.80	933.03	64.70	831.61	57.67
	Total area	1442	100	1442	100	1442	100

**Table 4** Accuracy assessment of LULC maps

Years	Classes	Built-up	Waterbody	Others	Row total	Producer accuracy (%)	User accuracy (%)	Overall accuracy (%)	Kappa coefficient
2001	Built-up	181	2	34	217	92.82	83.41	87.1	0.86
	Waterbody	2	68	10	80	89.47	85.00		
	Others	12	6	185	203	80.79	91.13		
	Column total	195	76	229	500	87.69	86.51		
2010	Built-up	221	0	16	237	90.57	93.25	88.61	0.89
	Waterbody	4	81	8	93	91.01	87.10		
	Others	19	8	143	170	85.63	84.12		
	Column total	244	89	167	500	89.07	88.15		
2016	Built-up	211	0	18	229	94.62	92.14	92.84	0.94
	Waterbody	0	98	6	104	98.00	94.23		
	Others	12	2	153	167	86.44	91.62		
	Column total	223	100	177	500	93.02	92.66		

images, an accuracy evaluation was conducted using an Error matrix. Table 4 depicts the accuracy assessment of classified images. Both producer and user accuracy of each class in all three years were more than 80 per cent. The overall accuracy was highest in 2016 with accuracy of 92.84% followed by 88.61% in 2010 and 87.10% in 2001. Similar trend was seen for kappa coefficient with 0.94 in 2016, 0.89 in 2010 and 0.86 in 2001, respectively.

### Urban footprint analysis

- The urban footprint, i.e. the influence that the expansions have on the conversion and transformation of character and identify of the surrounding areas is persuasive. It becomes increasingly easy to destroy green and rural areas in favour of urban functionalities and socio-physical identities.
- The rate of expansion is increasing. This is proven by the remote sensing analysis. If this is not stopped it is likely that other rural villages in the vicinity will be swallowed by this urban monster.
- The amount of green and open areas is rapidly decreasing, posing a big threat to liveability of the area, and possibly also food security provided by the surrounding rural areas.
- Agricultural areas are not replaced or re-located. Hence, there is going to be a problem finding suitable new agricultural areas.
- Water bodies are decreasing. This may provide significant problems from drinking water availability and irrigation in the near future.

All-in-all the figure depicts a situation of a rapidly deteriorating responsible use of land.

**Table 5** Area assessment of urban footprint classes

S. no	Class	Area in sq km		
		2001	2010	2016
1	Urban built-up	185.10	319.02	412.97
2	Suburban built-up	29.56	30.89	32.97
3	Rural built-up	94.95	45.65	28.06
4	Urbanized open land (UOL)	19.27	30.92	70.37
5	Captured open land (COL)	8.67	12.13	17.89
6	Rural open land (ROL)	59.04	47.68	32.56
7	Water	24.21	22.70	15.57
8	Others	1021.20	933.03	831.61
	Total	1442	1442	1442

Table 5 shows consistent rise in suburban area from 29.56 sq. km in 2001 to 32.97 sq. km in 2016. Similarly, open land was converted into other landuse for various purposes. In the span of fifteen years, it was observed that urban built-up has increased, while there was decline in rural area of GBN (Fig. 4).

### Temperature transition analysis

The advantage of thermal bands of satellite data is that LST can be estimated through the radiance values. During February 2001, the temperature ranged from 13.46 to 28.51 °C with a mean temperature of 20.98 °C.

During the year 2010, the temperature ranged from 17.45 to 32.31 °C with a mean LST of 24.88 °C. Later, in the year 2016, LST ranged between 20.10 and 36.42 °C with a mean of 28.26 °C (Fig. 5). The LST over the point of rural–urban transition was analysed indicating a rise in the temperature in the vicinity of those locations.



Fig. 4 Urban footprint analysis

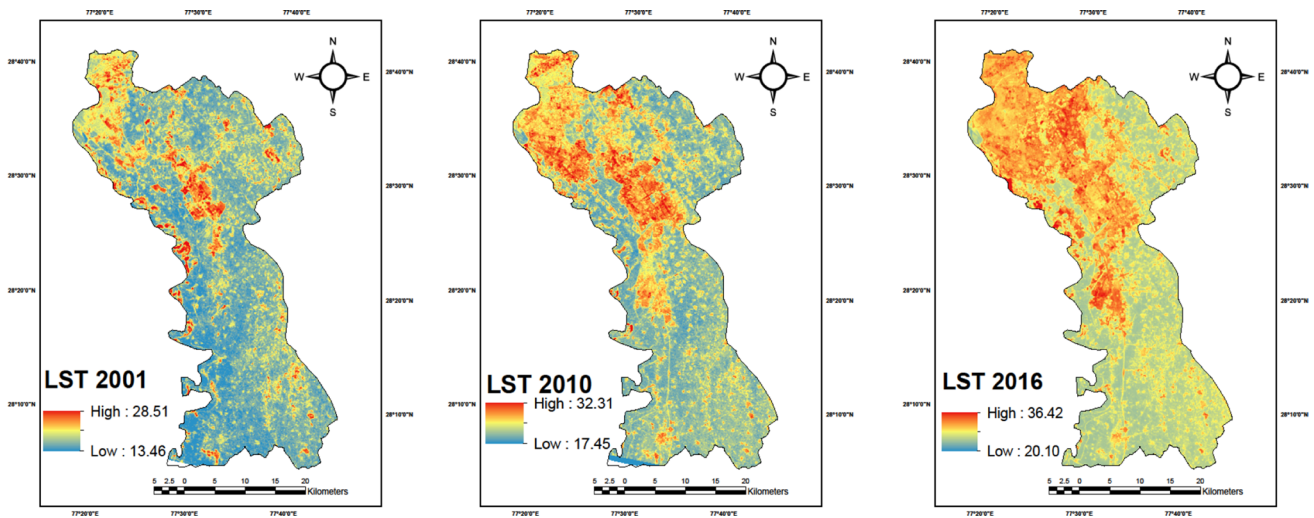
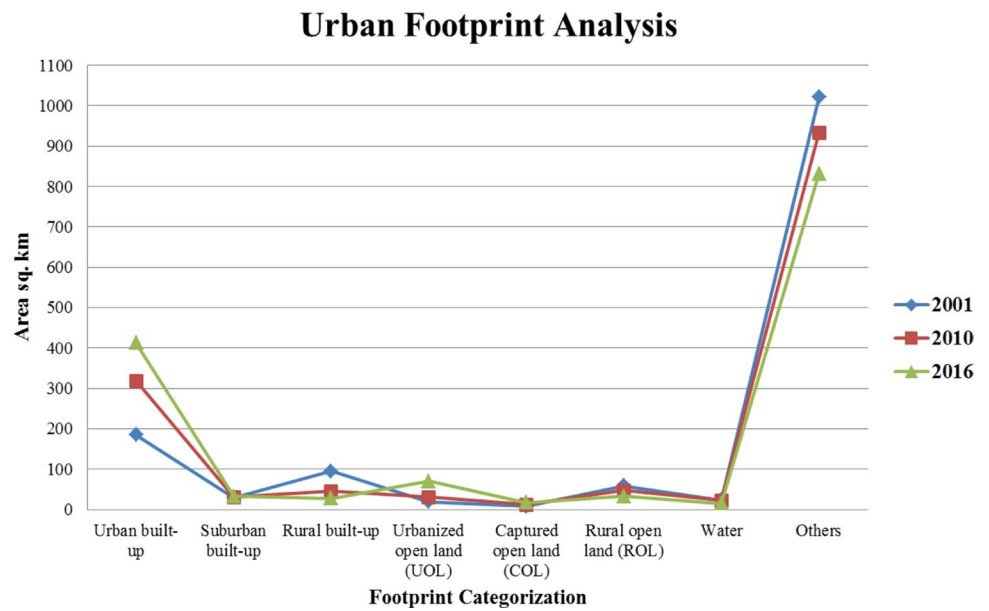
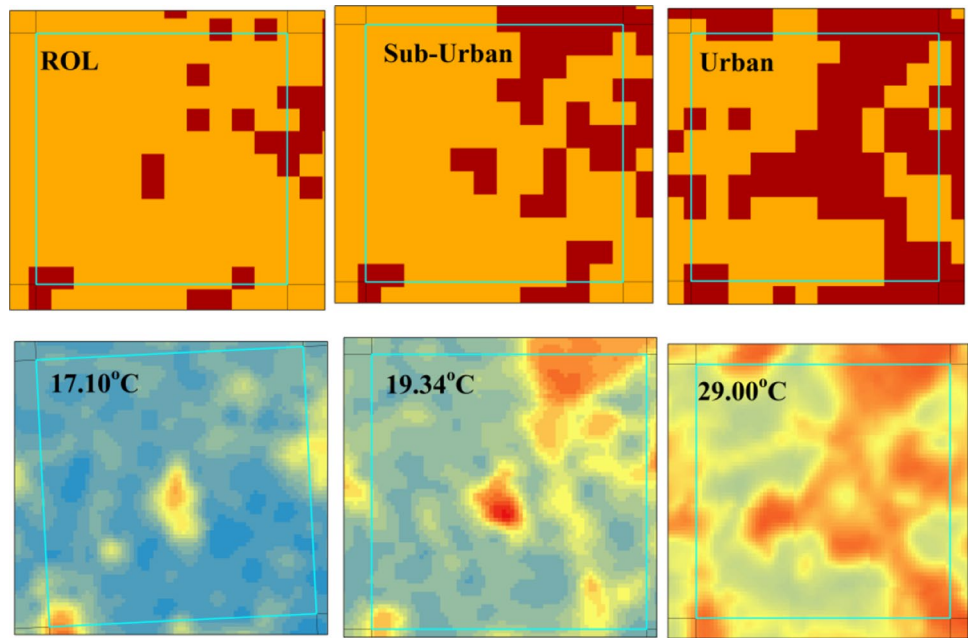


Fig. 5 Land surface temperature over a study area of 2001, 2010 and 2016

Table 6 Major transition locations over the study area that leads to the formation of urban heat islands

Transition locations	Footprint category 2001 → 2010 → 2016	LST (°C)		
		2001	2010	2016
Kherli Bhav Mozumpur	ROL → sub-urban → urban	17.1049	19.3452	29.0039
Jaypee sports city	UOL → urban → urban	16.3831	19.7885	29.4995
Jaganpur Doab	Rural → sub-urban → urban	16.1679	18.9897	28.2631
Sector 143 A, Noida	COL → UOL → urban	16.8479	19.881	28.6465
Greater Noida Zeta 2	COL → UOL → UOL	19.6729	20.7476	28.8092
Jalpura	COL → COL → urban	17.4320	18.8196	29.1493
DhoomManikpur	COL → UOL → urban	17.5129	19.2599	28.4967
Kudi Khera	Rural → sub-urban → sub-urban	19.3634	19.2456	27.6645
Chhapraula	Sub-Urban → urban → urban	18.6259	20.5426	29.3272
Bamheta village	Rural → rural → urban	15.7100	18.5132	29.354

**Fig. 6** Example of a grid (Kherli Bhav Mozumpur) depicting the formation of UHI in accordance with footprint category

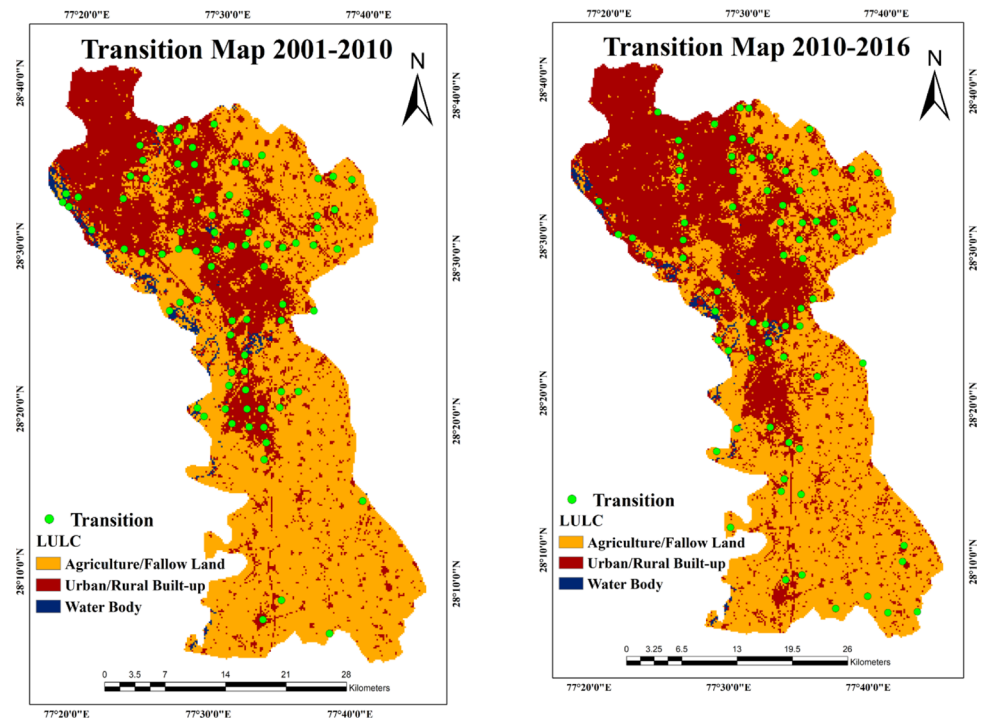


The elevated temperature and density of imperviousness in the study area result in the emergence of urban heat islands (UHI) as shown in Table 6 and Fig. 6. The point with less or no change in the land use pattern indicated a very less increment in temperature. The population outburst and urban expansion have resulted in an overall increase in LST over the study area.

### Driving factors of transition

The expansion and development of the study were done for the two time periods 2001–2010 and 2010–2016. By utilizing the results of urban footprint mapping and its attribute change, the transition points have been demarcated over the two time periods, as shown in Fig. 7. The unrestricted growth of core urban area towards the periphery or around a particular area leads to the transition of rural or open land

**Fig. 7** Urban–rural transition point a 2001–2010 b 2010–2016





into sub-urban and urban area. To assess the driving factors of transition the sub-category attributes were analysed and points of transition were demarcated.

The pattern of transition points indicates that within the study area, two types of urban expansion exist, i.e. a low density expansion that seems to be caused by an outward spreading of low-density sub-urban activities. The second type of urban expansion is a ribbon-shaped spatial sprawl, which can be characterized by enlargement of urban land ceilings along the major transportation lines. The low density expansion is prominent in the northern part of the study area, where controlled urban settlements were planned and built. This reflects the construction of planned residential areas as well as the gradual expansion or possibly redevelopment of once rural areas. In contrast, the urban socioeconomic activities and interdependencies along the Yamuna expressway roadways are reflected in the ribbon-shaped expansion.

## Conclusion

The study examines spatial patterns and changes in urban areas, revealing a sprawling nature of urbanization. From 2001 to 2016, suburban and urban built-up areas increased, while rural built-up areas decreased. This expansion is influenced by two types: low-density fragmented expansion and ribbon-shaped expansion. Low-density expansion may reflect socio-economic changes, such as gentrification and illegal occupation. Ribbon-shaped expansion represents increased socio-economic activities, which require access to transportation networks. This suggests that GBN is accommodating population beyond its carrying capacity, causing environmental degradation and increasing land surface temperature (LST). The findings suggest that urban development and expansion should be planned and managed sustainably. This integrated method can provide planners and policymakers with detailed insights into long-term trends, aiding in informed spatial decisions and better managing rural–urban transitions.

## Declarations

**Conflict of interest** The authors declare that they have no known competing financial interests or personal relationships that could have appeared to influence the work reported in this paper.

## References

- Anane GK (2022) Continuity in transition: spatial transformation in peri-urbanisation in Kumasi. *SN Social Sciences* 2(10):1–32. <https://doi.org/10.1007/s43545-022-00535-0>
- Angel S, Parent J, Civco D (2007) Urban sprawl metrics: an analysis of global urban expansion using GIS. In: *American society for photogrammetry and remote sensing-ASPRS annual conference 2007: identifying Geospatial Solutions*, vol 1, p 22–33. <https://nyuscholars.nyu.edu/en/publications/urban-sprawl-metrics-an-analysis-of-global-urban-expansion-using>
- Anugya Kumar V, Jain K (2017) Site suitability evaluation for urban development using remote sensing, GIS and analytic hierarchy process (AHP). *Adv Intell Syst Comput* 460:377–388. [https://doi.org/10.1007/978-981-10-2107-7\\_34](https://doi.org/10.1007/978-981-10-2107-7_34)
- Balha A, Singh CK (2018) Urban growth and management in Lucknow city the capital of Uttar Pradesh. *Geospatial applications for natural resources management*. CRC Press, Boca Raton, pp 109–122. <https://doi.org/10.1201/b22040-7>
- Bhatta B, Saraswati S, Bandyopadhyay D (2010) Urban sprawl measurement from remote sensing data. *Appl Geogr* 30(4):731–740. <https://doi.org/10.1016/j.apgeog.2010.02.002>
- Chen XL, Zhao HM, Li PX, Yin ZY (2006) Remote sensing image-based analysis of the relationship between urban heat island and land use/cover changes. *Remote Sens Environ* 104(2):133–146. <https://doi.org/10.1016/j.rse.2005.11.016>
- Cheng J, Masser I (2003) Urban growth pattern modeling: a case study of Wuhan city. *PR China Landsc Urb Plan* 62(4):199–217. [https://doi.org/10.1016/S0169-2046\(02\)00150-0](https://doi.org/10.1016/S0169-2046(02)00150-0)
- Congalton RG (1991) A review of assessing the accuracy of classifications of remotely sensed data. *Remote Sens Environ* 37(1):35–46. [https://doi.org/10.1016/0034-4257\(91\)90048-B](https://doi.org/10.1016/0034-4257(91)90048-B)
- Dhanaraj K, Angadi DP (2022) Geospatial analysis of contemporary urbanisation and rural–urban transition in Mangaluru. *India Asia-Pacific J Reg Sci* 6(2):515–539. <https://doi.org/10.1007/s41685-022-00239-6>
- Fazal S (2000) Urban expansion and loss of agricultural land - a GIS based study of Saharanpur city. *India Environ Urban* 12(2):133–149. <https://doi.org/10.1177/095624780001200211>
- Guo Y, Zhong W (2023) Rural transformation development and its influencing factors in China's poverty-stricken areas: a case study of Yanshan-Taihang mountains. *Land* 12(5):1080. <https://doi.org/10.3390/LAND12051080>
- Jat MK, Garg PK, Khare D (2008) Monitoring and modelling of urban sprawl using remote sensing and GIS techniques. *Int J Appl Earth Obs Geoinf* 10(1):26–43. <https://doi.org/10.1016/j.jag.2007.04.002>
- Jeganathan A, Andimuthu R, Prasannavenkatesh R, Kumar DS (2016) Spatial variation of temperature and indicative of the urban heat island in Chennai metropolitan area. *India Theoretical and Applied Climatology* 123(1–2):83–95. <https://doi.org/10.1007/s00704-014-1331-8>
- Ji W, Ma J, Twibell RW, Underhill K (2006) Characterizing urban sprawl using multi-stage remote sensing images and landscape metrics. *Comput Environ Urban Syst* 30(6):861–879. <https://doi.org/10.1016/j.compenvurbsys.2005.09.002>
- Jiang F, Liu S, Yuan H, Zhang Q (2007) Measuring urban sprawl in Beijing with geo-spatial indices. *J Geog Sci* 17(4):469–478. <https://doi.org/10.1007/s11442-007-0469-z>
- Kassouri Y, Okunlola OA (2022) Analysis of spatio-temporal drivers and convergence characteristics of urban development in Africa. *Land Use Policy* 112:105868. <https://doi.org/10.1016/j.landusepol.2021.105868>
- Kumar JAV, Pathan SK, Bhandari RJ (2007) Spatio-temporal analysis for monitoring urban growth—a case study of Indore City. *Journal of the Indian Society of Remote Sensing* 35(1):11–20. <https://doi.org/10.1007/BF02991829>
- Kumari M, Sarma K (2017) Changing trends of land surface temperature in relation to land use/cover around thermal power plant in Singrauli district, Madhya Pradesh. *India Spat Inf Res* 25(6):769–777. <https://doi.org/10.1007/s41324-017-0142-2>



- Lillesand TM, Kiefer RW (1979) Remote sensing and image interpretation. In: Remote sensing and image interpretation. Wiley & Sons, New Jersey. <https://doi.org/10.2307/634969>
- Martinuzzi S, Gould WA, Ramos González OM (2007) Land development, land use, and urban sprawl in Puerto Rico integrating remote sensing and population census data. *Landsc Urban Plan* 79(3–4):288–297. <https://doi.org/10.1016/j.landurbplan.2006.02.014>
- Mushore TD, Odindi J, Dube T, Matongera TN, Mutanga O (2017) Remote sensing applications in monitoring urban growth impacts on in-and-out door thermal conditions: A review. In: Remote Sensing Applications: Society and Environment. vol 8, p. 83–93. <https://doi.org/10.1016/j.rsase.2017.08.001>
- Niyogi D, Subramanian S, Mohanty UC, Kishtawal CM, Ghosh S, Nair US, Ek M, Rajeevan M (2018) The impact of land cover and land use change on the indian monsoon region hydroclimate. p 553–575. [https://doi.org/10.1007/978-3-319-67474-2\\_25](https://doi.org/10.1007/978-3-319-67474-2_25)
- Ren Z, He X, Zheng H, Zhang D, Yu X, Shen G, Guo R (2013) Estimation of the relationship between urban park characteristics and park cool island intensity by remote sensing data and field measurement. *Forests* 4(4):868–886. <https://doi.org/10.3390/f4040868>
- Roy B, Kasemi N (2021) Monitoring urban growth dynamics using remote sensing and GIS techniques of Raiganj urban agglomeration, India. *Egypt J Remote Sens Space Sci* 24(2):221–230. <https://doi.org/10.1016/j.ejrs.2021.02.001>
- Somvanshi SS, Kumari M (2020) Comparative analysis of different vegetation indices with respect to atmospheric particulate pollution using sentinel data. *Appl Comput Geosci* 7:100032. <https://doi.org/10.1016/j.acags.2020.100032>
- Somvanshi SS, Bhalla O, Kunwar P, Singh M, Singh P (2020) Monitoring spatial LULC changes and its growth prediction based on statistical models and earth observation datasets of Gautam Budh Nagar, Uttar Pradesh, India. *Environ Dev Sustain* 22(2):1073–1091. <https://doi.org/10.1007/s10668-018-0234-8>
- Stabursvik EM (2007) The challenge of identifying and conserving valuable ecosystems close to human settlements in a northern area. <http://munin.uit.no/bitstream/handle/10037/1205/thesis.pdf?sequence=4>
- Stone B, Hess JJ, Frumkin H (2010) Urban form and extreme heat events: are sprawling cities more vulnerable to climate change than compact cities? *Environ Health Perspect* 118(10):1425–1428. <https://doi.org/10.1289/ehp.0901879>
- Sudhira HS, Ramachandra TV, Jagadish KS (2004) Urban sprawl: metrics, dynamics and modelling using GIS. *Int J Appl Earth Obs Geoinf* 5(1):29–39. <https://doi.org/10.1016/j.jag.2003.08.002>
- Tang J, Wang L, Yao Z (2007) Spatio-temporal urban landscape change analysis using the Markov chain model and a modified genetic algorithm. *Int J Remote Sens* 28(15):3255–3271. <https://doi.org/10.1080/01431160600962749>
- Tsai YH (2005) Quantifying urban form: compactness versus “sprawl.” *Urban Studies* 42(1):141–161. <https://doi.org/10.1080/0042098042000309748>
- Zhang S, Zhao J, Jiang Y, Cheshmehzangi A, Zhou W (2023) Assessing the rural–urban transition of China during 1980–2020 from a coordination perspective. *Land* 12(6):1175. <https://doi.org/10.3390/land12061175>
- Zhao S, Feng T, Tie X, Dai W, Zhou J, Long X, Li G, Cao J (2019) Short-Term weather patterns modulate air quality in eastern China during 2015–2016 winter. *J Geophys Res: Atmos* 124(2):986–1002. <https://doi.org/10.1029/2018JD029409>

Springer Nature or its licensor (e.g. a society or other partner) holds exclusive rights to this article under a publishing agreement with the author(s) or other rightsholder(s); author self-archiving of the accepted manuscript version of this article is solely governed by the terms of such publishing agreement and applicable law.

